https://doi.org/10.5194/acp-2019-933
Preprint. Discussion started: 9 January 2020

Atmospheric Chemistry and Physics Discussions

Simultaneous Measurement of Urban and Rural Single Particles in Beijing, Part I: Chemical Composition and Mixing State

Yang Chen[1], Jing Cai[2], Zhichao Wang[1], Chao Peng[1], Xiaojiang Yao[1], Mi Tian[1], Yiqun Han[2], Guangming Shi[1,3], Zongbo Shi[4,5], Yue Liu[2], Xi Yang[2], Mei Zheng[2*], Tong Zhu[2], Kebin He[6], Qiang Zhang[7], and Fumo Yang[3,1*]

[1]Center for the Atmospheric Environment Research, Chongqing Institute of Green and Intelligent Technology, Chinese Academy of Sciences, Chongqing 400714, China

[2] SKL-ESPC and BIC-ESAT, College of Environmental Sciences and Engineering, Peking University, Beijing 100871, China

[3]College of Architecture and Environment, Sichuan University, Chengdu 610065, China

[4] School of Geography Earth and Environmental Sciences, University of Birmingham, Birmingham B15 2TT, UK

[5]Institute of Surface-Earth System Science, Tianjin University, Tianjin 300072, China

[6] School of Environment, Tsinghua University, Beijing 100084, China

[7]Department of Earth System Science, Tsinghua University, Beijing, China

Corresponding to Fumo Yang (fmyang@scu.edu.cn) and Mei Zheng (mzheng@pku.edu.cn)

Keywords: urban; regional; single particle; transport; mixing state

https://doi.org/10.5194/acp-2019-933
Preprint. Discussion started: 9 January 2020

Atmospheric Chemistry and Physics Discussions

Abstract

Two single particle aerosol mass spectrometers (SPAMS) were deployed simultaneously at an urban and a rural site in Beijing during an intensive field campaign from 1st to 29th Nov 2016 to investigate the source and process of airborne particles in Beijing. In the first part of this research, we report the single-particle chemical composition, mixing state, and evolution at both sites. 96% and 98% of collected particles were carbonaceous at the urban and rural sites, respectively. Five particle categories, including elemental carbon (EC), organic carbon (OC), internal-mixed EC and OC (ECOC), potassium-rich (K-rich), and Metals were observed at both sites. The categories were partitioned into particle types depending on different atmospheric processing stages. Seventeen particle types were shared at both sites. In the urban area, nitrate-containing particle types, such as EC-Nit and ECOC-Nit, were enriched, especially at night; sulfate-containing particles were transported when wind speed was high; ECOC-Nit-Sul were mostly local-aged. In sum, these processed particles took up to 85.3% in the urban areas. In the rural area, regional particles were abundant, but freshly emitted ECOC and OC had distinct patterns that were pronounced at cooking and heating time. Biomass burning, traffic, and coal burning were major sources of $PM_{2.5}$ in both rural and urban areas. Besides, the particles from the steel industry located in the south were also identified. In summary, the chemical composition of urban and rural particle types was similar in Beijing; the urban particles were influenced significantly by rural processing and transport. The work is useful to understand the evolution of urban and rural particles in Beijing during winter.

https://doi.org/10.5194/acp-2019-933
Preprint. Discussion started: 9 January 2020

1. Introduction

China has experienced severe haze events caused by extremely high concentrations of fine particulate matter ($PM_{2.5}$) since January 2013. In the worst cases, an area of 2.0 million km^2 and a population of 800 million were affected (Huang et al., 2014). In the Beijing-Tianjin-Hebei (BTH) area, extreme haze events frequently occur during winter, with $PM_{2.5}$ mass reaching rapidly up to 200 μg m^{-3} and sustaining such levels for hours (Guo et al., 2014).

Over the last two decades, comprehensive studies have been conducted on urban PM in Beijing. He et al. (2001) reported the first characterization of $PM_{2.5}$. Since then, numerous studies have been published on characterization (Huang et al., 2010), sources (Guo et al., 2012; Sun et al., 2014), and processing of PM (Sun et al., 2013). The mechanism of rapid-boosting $PM_{2.5}$ in Beijing, including new particle formation and growth (Guo et al., 2014), regional transport (Li et al., 2015), and both (Du et al., 2017; Sun et al., 2014), have been proposed. However, discrepancies remain among these studies.

Single particle mass spectrometers (SPMS) have been used to investigate the size-resolved chemical composition and mixing state of atmospheric particles (Gard et al., 1997; Pratt and Prather, 2012). More recently, single particle aerosol mass spectrometers (SPAMS) have been used in Chinese megacities such as Beijing (Li et al., 2014), Shanghai (Tao et al., 2011), Guangzhou (Bi et al., 2011), Xi'an (Chen et al., 2016), Nanjing (Wang et al., 2015), and Chongqing (Chen et al., 2017).

https://doi.org/10.5194/acp-2019-933
Preprint. Discussion started: 9 January 2020

Atmospheric Chemistry and Physics Discussions

In Beijing, particle types, such as carbonaceous, metal, dust, K-rich, and others during spring and fall, were reported (Liu et al., 2016b; Li et al., 2014). Besides, lead-containing particles have also been investigated in recent studies (Ma et al., 2016; Cai et al., 2017). However, due to the insufficient consideration of mixing state of nitrate, sulfate, and organics, these studies paid limited attention to the atmospheric particulate processing.

This study is a part of the APHH-Beijing (Atmospheric Pollution and Human Health in a Chinese Megacity of Beijing) intensive field campaign during winter 2016 (Shi et al., 2019). Two SPAMSs were deployed simultaneously at Peking University (PKU) and Pinggu (PG) in order to observe both urban and rural particles in the Beijing region. The aims of the study are 1) to characterize the single-particle chemical composition and mixing state; 2) to investigate particulate evolution at both sites during haze events. These two objectives are presented in two parts. In Part I, particle types and their atmospheric processing (e.g., origination, source, and diurnal profiles) at both sites are reported; in Part II, the detailed analysis of haze events, effects of heating activities, and evidence of regional transport are addressed.

2. Methodology

2.1 Sampling sites

The campaigns were performed simultaneously at PKU (116.32ºE, 39.99ºN) and PG (117.05ºE, 40.17ºN) from 11/01/2016 to 11/29/2016. A Description of the PKU site is available in the literature (Huang et al., 2006). Briefly, the site is located on the rooftop (15 m above the ground) on the PKU campus which is surrounded by residential and

https://doi.org/10.5194/acp-2019-933
Preprint. Discussion started: 9 January 2020

commercial blocks. Trace gases (Thermo Inc. series), meteorological parameters (Vaisala Inc.), and $PM_{2.5}$ (TEOM 1430) were recorded during the observation.

The PG site (117.053ºE, 40.173ºN) is 3 km from the PG center. The site is located in the northeast of the PKU site with a distance of 70 km. The PG site also acts as a host of the AIRLESS (Effects of AIR pollution on the cardiopulmonary disease in urban and peri-urban residents in Beijing) Project. The meteorological data is acquired from the local meteorological office. The PG village is surrounded by orchards and farmland with no main road nearby on a scale of 3 km. Coal and biomass are used for domestic heating and cooking in the nearby villages.

2.2 Instrumentation and data analysis

Two SPAMSs (Model 0515, Hexin Inc., Guangzhou, China) were deployed at both PKU and PG. A technical description of SPAMS is available in (Li et al., 2011). Briefly, a SPAMS has three functional parts: sampling, sizing, and mass spectrometry. In the sampling part, particles within a 0.1–2.0 μm size range pass efficiently through an aerodynamic lens. In the sizing unit, the aerodynamic diameter (D_{va}) is calculated using the time-of-flight of particles. The particles are then decomposed and ionized into ions one-by-one using a 266 nm laser. A bipolar time-of-flight mass spectrometer measures the ions and generates the positive and negative mass spectra of each particle. The two instruments were maintained and calibrated following the standard procedures before sampling (Chen et al., 2017).

https://doi.org/10.5194/acp-2019-933
Preprint. Discussion started: 9 January 2020

A neural network algorithm based on adaptive resonance theory (ART-2a) was used to resolve particle types from both datasets (Song et al., 1999). The parameters used were: a vigilance factor of 0.70, a learning rate of 0.05, and 20 iterations. This procedure generated 771 and 792 particle groups. Then, the groups were combined into particle types based on similar mass spectra, temporal trends, and size distributions (Dallosto and Harrison, 2006). During combining, relative areas of nitrate and sulfate were used to distinguish the stages of processing, assuming that more sulfate and nitrate can be measured if a particle is more processed during its lifetime. Thus, particles with relative peak areas of sulfate and nitrate larger than 0.1 were marked with nitrate (-Nit), sulfate (-Sul), respectively, or both. Finally, the strategy resulted in 20 and 19 particle types at PKU and PG respectively. Among them, 17 types appeared at both sites, and each type has identical mass spectra (R^2> 0.80) between each other.

3. Results

A total of 4,499,606 and 4,063,522 particles were collected at PKU and PG sites, respectively. The size distributions peaked at 0.48 μm and 0.52 μm (Figure 1). The smaller size distribution was due to a more substantial fraction of freshly-emitted particles at PG, as described in Table 1. Seventeen particle types (R^2 > 0.80, mass spectra) were observed both at PKU and PG (Table 1). These particle types were labeled with the suffixes "_PKU" or "_PG" to indicate their locations. The term "particle category" stands for a group of particle types with variable stages of processing.

https://doi.org/10.5194/acp-2019-933
Preprint. Discussion started: 9 January 2020

Atmospheric Chemistry and Physics Discussions

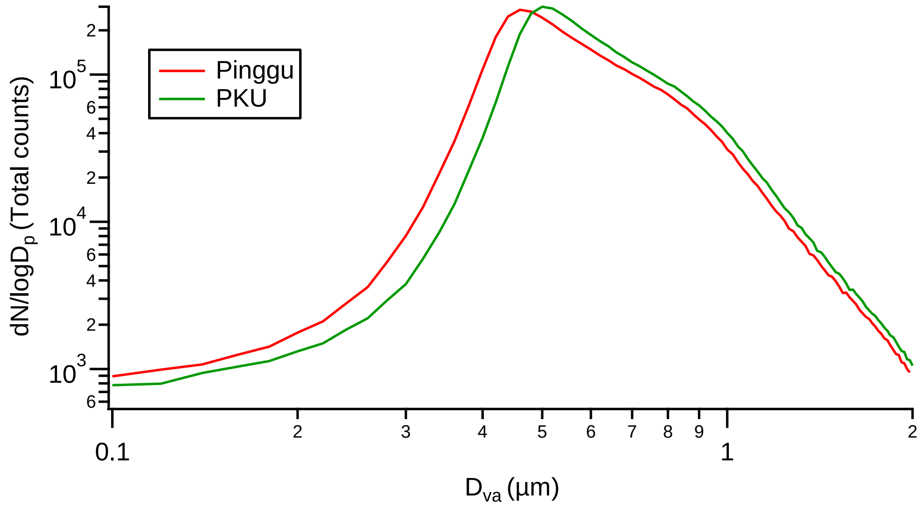

Figure 1. The size distribution of SPAMS particles at PKU and PG sites.

https://doi.org/10.5194/acp-2019-933
Preprint. Discussion started: 9 January 2020

Table 1. SPAMS particle types identified at PKU and PG sites.

At both sites	Particle type	PKU Number	PKU Percentage	PG Number	PG Percentage
EC	EC-Nit	313574	7.0	79082	2.0
	EC-Nit-Sul	473908	10.5	140107	3.5
	EC-Sul	30365	0.7	4096	0.1
	ECOC-Nit-Sul	539533	12.0	755279	18.6
	ECOC-Sul	572548	12.7	397367	9.8
K-rich	K-rich	322731	7.2	259287	6.4
	K-Nit	359281	8.0	334547	8.2
	K-Nit-Sul	717280	16.0	76954	1.9
	K-Sul	26301	0.6	183571	4.5
NaK	NaK	16680	0.4	74943	1.8
	NaK-Nit	289259	6.4	69760	1.7
	NaK-Nit-Sul	114387	2.5	77555	1.9
	NaK-Sul	7509	0.2	16578	0.4
OC	OC-Nit-Sul	334870	7.4	865821	21.3
	OC-Sul	40800	0.9	279322	6.9
	Ca-dust	19869	0.4	3035	0.1
Metal	Fe-rich	137600	3.1	70920	1.8
	ECOC-Nit	137470	3.1%		
	OC-Nit	41159	0.9%		
	K-Amine-Nit-Sul	4482	0.1%		
	ECOC			239953	5.9%
	OC			135345	3.3%

Note: Nit stands for nitrate, Sul for sulfate.

3.1 Meteorological conditions and overview

Temperature, relative humidity (RH), and wind speed at both sites during the sampling period are summarized in Table 2. Their temporal trends are available in Part II. The average temperature at PKU (urban, 5.7±2.3 °C) was higher than at PG (rural, 3.1±2.2 °C). Correspondingly, relative humidity was higher at PG (67±32%) than at PKU (49±30%). The wind was stronger at PKU (2.5± 1.8 ms^{-1}) than at PG (1.7± 0.9 ms^{-1}). As shown in

https://doi.org/10.5194/acp-2019-933
Preprint. Discussion started: 9 January 2020

Figure 2, at PKU, wind speed peaked at noon (local time, UTC+8), while at PG, wind speed reached its maxima at 15:00. Various wind speeds determined the different dispersion patterns of pollutants near the surface. It should be noticed that wind speed up to 2 ms^{-1} representing a scale of 172 km in diurnal transport. Therefore, at PKU, the wind could bring the pollutants from Hebei province under stagnant air conditions.

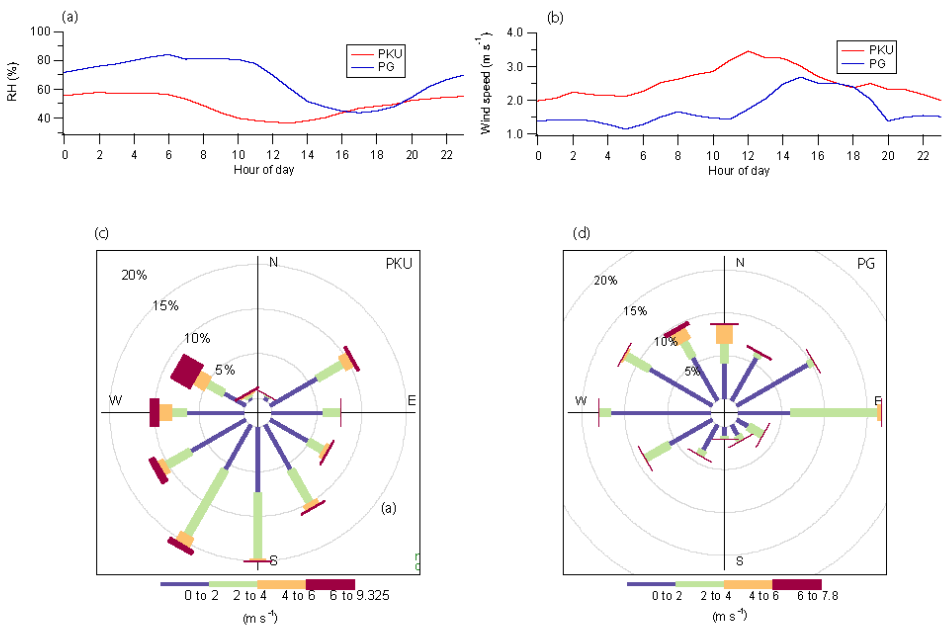

Figure 2. Diurnal plots of (a) RH and (b) wind speed, and rose plots of wind at (c)PKU and (d) PG.

Table 2. Meteorological parameters at PKU and PG during the campaign.

	PKU	PG
Temperature (°C)	5.7±2.3	3.1±2.2
RH (%)	49±30	67±32
Wind speed (ms^{-1})	2.5± 1.8	1.7± 0.9

https://doi.org/10.5194/acp-2019-933
Preprint. Discussion started: 9 January 2020

Atmospheric Chemistry and Physics
Discussions

3.2 Common particle categories at both PKU and PG

3.2.1 Elemental carbon (EC)

As shown in Figure 3a, the elemental carbon (EC) particle category was represented by ions peaking at *m/z* 12, 24, 36, 48, and 60 in positive mass spectra (Sodeman et al., 2005; Toner et al., 2008). EC is emitted from solid fuel combustion, traffic (Sodeman et al., 2005; Toner et al., 2008; Toner et al., 2006), and industrial activities (Healy et al., 2012). Due to the various ionic intensities of nitrate (*m/z* -46 and -62) and sulfate (*m/z* -80 and -97), the EC category has four types including EC-Nitrate (EC-Nit), EC-Sulfate (EC-Sul), and EC-Nit-Sul. Besides, the EC category was more abundant after the heating began rather than before (Part II), indicating that coal burning was one of the primary sources.

EC-Nit_PKU and EC-Nit_PG accounted for 7.0% and 2.0% in PKU and PG datasets, respectively. In the diurnal profiles of EC-Nit_PKU, there was an apparent early morning peak at 5:00 (UTC+8, local time), along with an evening peak (22:00). There was also an early morning NO_x peak in the urban area of Beijing, providing sufficient precursors for secondary nitrate (Shi et al., 2019). Wang et al. (2018) validated the role of N_2O_5 uptake on the nitrate formation in PM. Therefore, the early morning peak of EC-Nit_PKU occurred due to the uptake of nitrate on the freshly emitted EC in the early morning (Sun et al., 2014). The evening peak could be due to the low temperature after the heating supply started. Diurnally, EC-Nit_PG exhibited an early morning peak (5:00) but no evening peak and mainly came from the southeast.

EC-Nit-Sul was more abundant at the rural site (18.6%) than the urban site (11.6%). EC-Nit-Sul_PKU (10.5%) had early morning (04:00), morning (7:00), and afternoon peaks

https://doi.org/10.5194/acp-2019-933
Preprint. Discussion started: 9 January 2020

(around 16:00), while EC-Nit-Sul_PG (3.5%) had early morning (04:00), noon, and afternoon peaks (17:00, Figure 3a). However, they showed relatively small diurnal variations. For example, EC-Nit-Sul_PKU varied between 800 h^{-1} and 1,000 count h^{-1}, and EC-Nit-Sul_PG shifted between 200 count h^{-1} and 250 count h^{-1}. Thus, the EC-Nit-Sul at both sites was most likely acting as background and regional particles (Dall'Osto et al., 2016). Additionally, EC-Nit-Sul_PKU mainly came from the surrounding area in the city pollutant plume, while EC-Nit-Sul_PG mainly came from the southeast (Figure 3c).

EC-Sul was a minor type at both sites, accounting for 0.7% at PKU and 0.1% at PG. EC-Sul was pronounced in the afternoon when the wind was strong at both sites. It was unlikely for either EC-Sul_PKU or EC-Sul_PG to be local because their concentrations were associated with high wind speed, as shown in Figure 3c. More specifically, EC-Sul_PKU came from the southeast and northeast of Hebei Province when the wind speed exceeded 6 m s^{-1}. EC-Sul_PG could come from the west when the wind speed exceeded 2 m s^{-1} and the east when the wind speed exceeded 3 m s^{-1}, as coal-using industries are located in both directions. Also, at both sites, the concentrations of SO_2 were elevated in the afternoon due to transport, providing sufficient precursors for the formation of sulfate (Shi et al., 2019).

https://doi.org/10.5194/acp-2019-933
Preprint. Discussion started: 9 January 2020

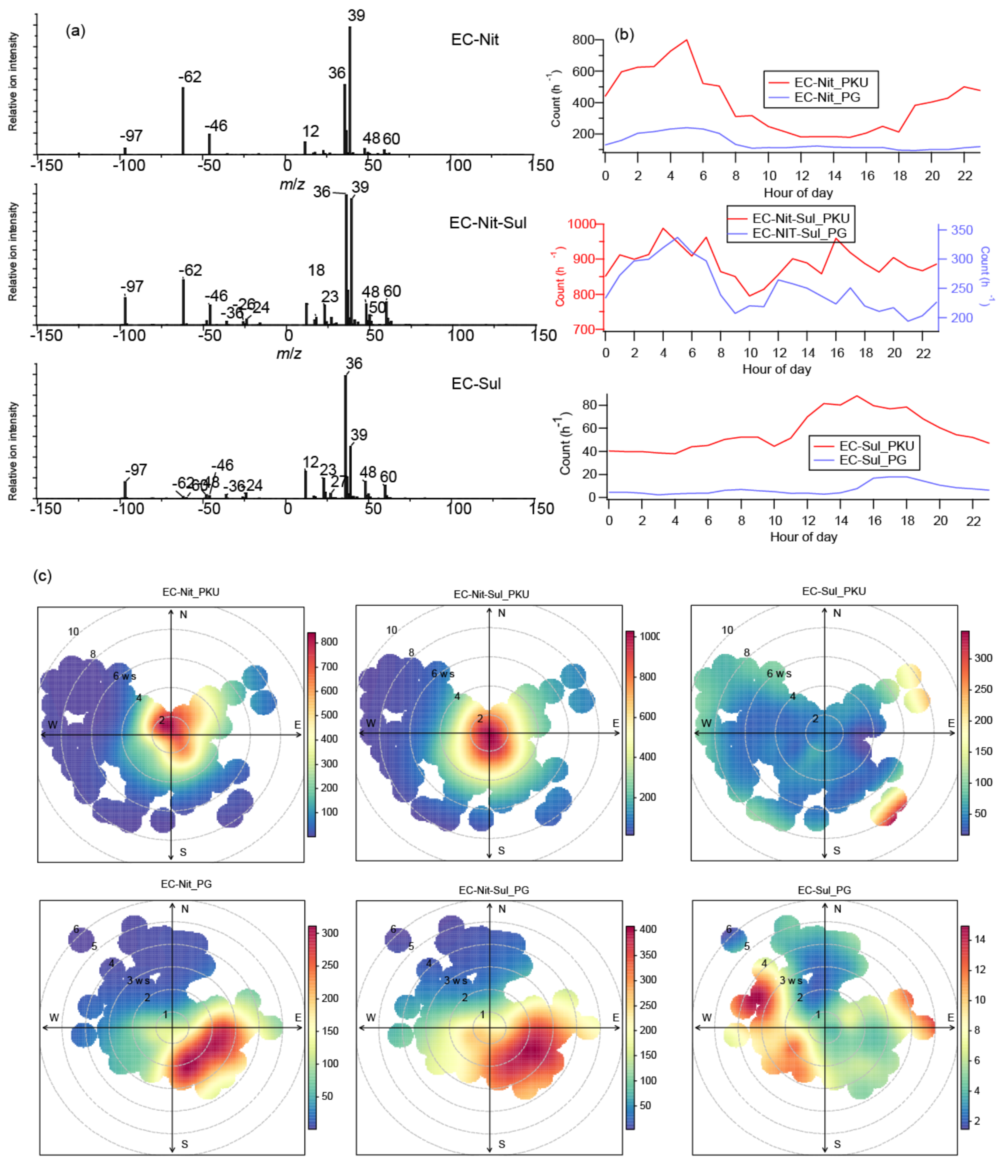

Figure 3. (a) average mass spectra of EC-Nit, EC-Nit-Sul, and EC-Sul at both sites; (b) diurnal patterns of EC-Nit, EC-Nit-Sul, and EC-Sul at both sites; (c) polar plots of EC-Nit, EC-Nit-Sul, and EC-Sul; the grey circles indicate wind speed (m s^{-1}).

3.2.2 Organic carbon (OC) category

The positive mass spectra of both OC-Nit and OC-Nit-Sul contained complicated organic ions such as $C_2H_3^+$ (*m/z* 27), C_3H^+ (*m/z* 37), $C_3H_7^+$/$C_2H_3O^+$/ $CHNO^+$ (*m/z* 43), $C_4H_2^+$ (*m/z* 50), aromatic hydrocarbons ($C_4H_3^+$, $C_5H_3^+$, and $C_6H_5^+$), and diethylamine ($(C_2H_5)_2NH_2^+$, *m/z* 74), $(C_2H_5)_2NCH_2^+$ (*m/z* 86)). The negative mass spectra contained CN^- (*m/z* –26), Cl^- (*m/z* –35 and 37), CNO^- (*m/z* –42), nitrate (*m/z* –46 and –62), and sulfate(*m/z* –97). The presence of CN^- and CNO^- suggests the existence of organonitrogen species (Day et al., 2010). Peak intensities of organic fragments are relatively high in the OC-Sul particles, indicating that it was relatively fresh, while OC-Nit-Sul was more processed (Zhai et al., 2015). The positive mass spectrum had similar ions of Coal Combustion OA (CCOA) with significant signals of PAHs in AMS studies (Sun et al., 2013). OC-Sul showed different spatial distributions with 0.9% at PKU and 6.9% at PG.

OC-Sul_PG had morning (8:00) and afternoon (16:00) peaks, while the diurnal profile of OC-Sul_PKU showed a trend with an early morning (3:00), morning (10:00), and afternoon peaks (16:00). The diurnal trends OC-Sul at both PKU and PG were consistent with the heating pattern depending on the variation of local temperature. Moreover, OC-Sul_PG increased after the heating supply began. Polar plots suggest that OC-Sul_PKU came from surrounding southwest areas via transport, while OC-Sul_PG came from villages to the east and west (Figure 4). These results suggest that OC-Sul_PG was emitted from coal burning for residential heating in nearby areas.

OC-Nit-Sul accounted for 7.4 % and 21.3 % of all detected particles at PKU and PG, respectively. OC-Nit-Sul_PKU had a diurnal peak at 7:00 in rush hours, suggesting that

https://doi.org/10.5194/acp-2019-933
Preprint. Discussion started: 9 January 2020

Atmospheric Chemistry and Physics
Discussions

OC-Nit-Sul could be formed due to the uptake of nitrate on OC-Sul. While OC-Nit-Sul_PG had a diurnal peak at 8:00 due to traffic in nearby towns. As an aged particle type, OC-Nit-Sul_PKU and OC-Nit-Sul_PG, also acting as a similar type of background types with hourly counts remained low but elevated to high levels at night. Polar plots suggest that OC-Nit-Sul_PKU mainly came from the surrounding areas, while OC-Nit-Sul_PG mainly came from the south and east, where populous villages are located (Figure 4).

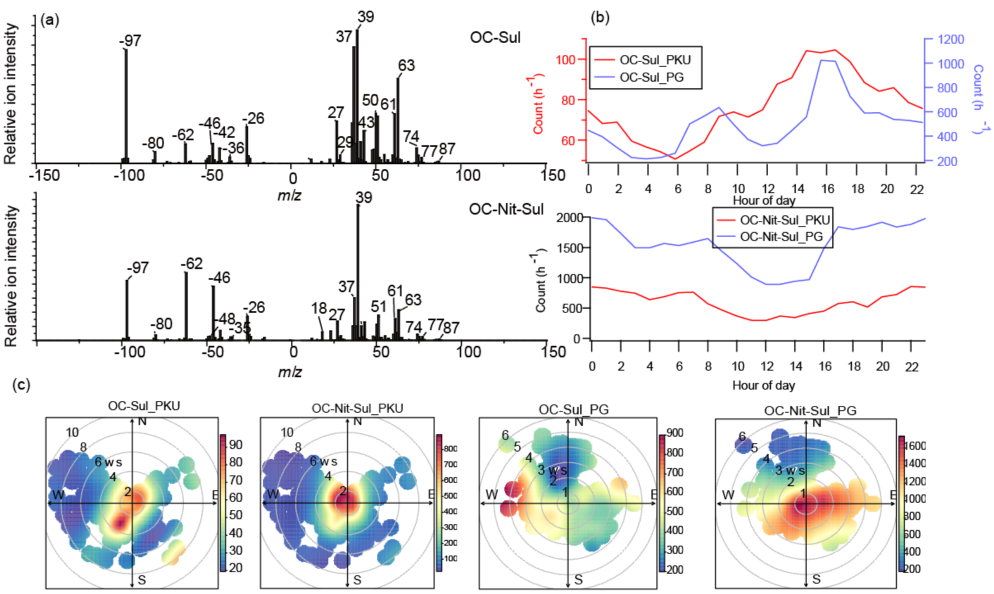

Figure 4. (a): average mass spectra of OC-Nit and OC-Nit-Sul observed at both sites; (b): diurnal patterns of the hourly count of OC-Nit and OC-Nit-Sul at both sites; (c): polar plots of OC-Sul and OC-Nit-Sul; the grey circles indicate wind speed (m s^{-1}).

3.2.3 ECOC category

As shown in Figure 5a, the ECOC category contained two major particle types: ECOC-Nit-Sul and ECOC-Sul. The positive mass spectrum of ECOC-Nit-Sul contained C_n^+ (*m/z*

https://doi.org/10.5194/acp-2019-933
Preprint. Discussion started: 9 January 2020

12, 24, 36…), NH_4^+ (*m/z* 18), $C_2H_3^+$ (*m/z* 27), K^+ (*m/z* 39 and 41), $C_3H_7^+/C_2H_3O^+/CHNO^+$ (*m/z* 43), $C_4H_2^+$ (*m/z* 50), and $[(C_2H_5)_2NH_2]^+$ (*m/z* 74); in the negative mass spectrum, ions such as sulfate (*m/z* -80 and -97), nitrate (*m/z* -46 and -62), C_n^-, and CN^- (*m/z* -26) were abundant. This mixture of EC and OC particle types was common in single particle studies. ECOC could be local, and from incomplete combustion processes (Chen et al., 2017), or regional transport, e.g., after aging (McGuire et al., 2011; Huang et al., 2013). The diurnal profile of ECOC-Sul_PG showed early morning (1:00), morning (8:00), and afternoon (17:00) peaks, which is consistent with local cooking and heating patterns. Also, heating activities enhanced the fraction of ECOC-Sul_PG. ECOC-Sul_PKU did not show a clear diurnal profile, suggesting that ECOC-Sul_PKU was mainly a background type. Similarly, ECOC-Nit-Sul_PKU and ECOC-Nit-Sul_PG were also background types with less obvious diurnal variations (Dall'Osto et al., 2016). Polar plots (Figure 5c) suggested that both ECOC-Nit-Sul_PKU and ECOC-Sul_PKU had both local and regional sources. Wind speed up to 4 m s^{-1} could cause a transport with a distance of 346 km diurnally, indicating that it was possible for the particles from Hebei province to arrive at the sampling place.

https://doi.org/10.5194/acp-2019-933
Preprint. Discussion started: 9 January 2020

Atmospheric Chemistry and Physics
Discussions

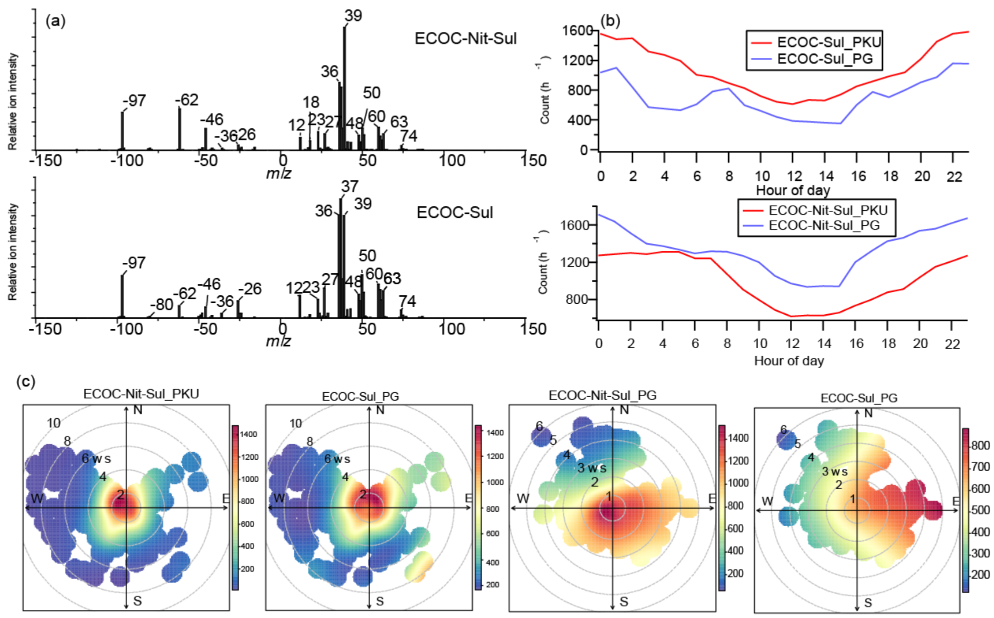

Figure 5. (a): average mass spectra of ECOC-Nit and ECOC-Nit-Sul observed at both sites; (b): diurnal patterns of the hourly count of ECOC-Sul and ECOC-Nit-Sul at both sites; (c): polar plots of ECOC-Sul and ECOC-Nit-Sul; the grey circles indicate wind speed (ms^{-1}).

3.2.4 K-rich category

Figure 6 shows a series of potassium-rich (K) particle types. K-rich contained Na^+ (*m/z* 23), $C_2H_3^+$ (*m/z* 27), C_n^+, C_3H^+ (*m/z* 37), K^+, aromatic hydrocarbons ($C_4H_3^+$, $C_5H_3^+$, and $C_6H_5^+$), levoglucosan (*m/z* -45, -59, and -71), sulfate, and nitrate. According to the ionic intensities of sulfate and nitrate, the K-rich particle category had several branches such as K-rich, K-Nit, K-Sul, and K-Nit-Sul. K-rich particles are commonly found in biomass burning emissions (Silva et al., 1999; Pagels et al., 2013; Chen et al., 2017). Cl^- was unabundant in all K-rich particle types, suggesting that the K-rich particles had undergone aging during

https://doi.org/10.5194/acp-2019-933
Preprint. Discussion started: 9 January 2020

atmospheric processing (Sullivan et al., 2007; Chen et al., 2016), but K-Nit, K-Nit-Sul, and K-Sul were more processed.

All K-rich category particles showed different atmospheric evolution process at both PKU and PG. K-rich_PKU illustrated a typical pattern that was at low levels in the daytime but high levels at nighttime (22:00). As shown in Figure 6c, at an average wind speed of 3 m s^{-1}, it took five hours for particles from a distance of 50 km to arrive at PKU. This is also the reason why BB-related particles were abundant in urban Beijing where the household BB is prohibited. The origination of K-rich_PKU was from nearby and southwest. K-rich_PG, however, showed a pattern with cooking and heating activities, peaking at 7:00 and 17:00. The peak at 7:00 was due to the local emissions; the 17:00 could be transported from a distance of 50 km at a wind speed of 3 m s^{-1} from the east and west.

The secondary process contributed to the early morning peak (5:00) of K-Nit_PKU due to the nighttime formation of nitrate via hydrolysis of N_2O_5 in the NO_x-rich urban areas (Wang et al., 2017). In the day time, after the rush hours, the number concentration of K-Nit_PKU increased again via the uptake of nitrate due to day time photoactivity. K-Nit_PKU mainly originated from the local and southerly areas (Figure 6c). Besides the early morning peak, K-Nit_PG showed cooking and heating patterns that they were abundant when the temperature was low in the early morning and afternoon. K-Nit_PG had wide originated from both local and region via long-range transport.

https://doi.org/10.5194/acp-2019-933
Preprint. Discussion started: 9 January 2020

Atmospheric Chemistry and Physics
Open Access
Discussions

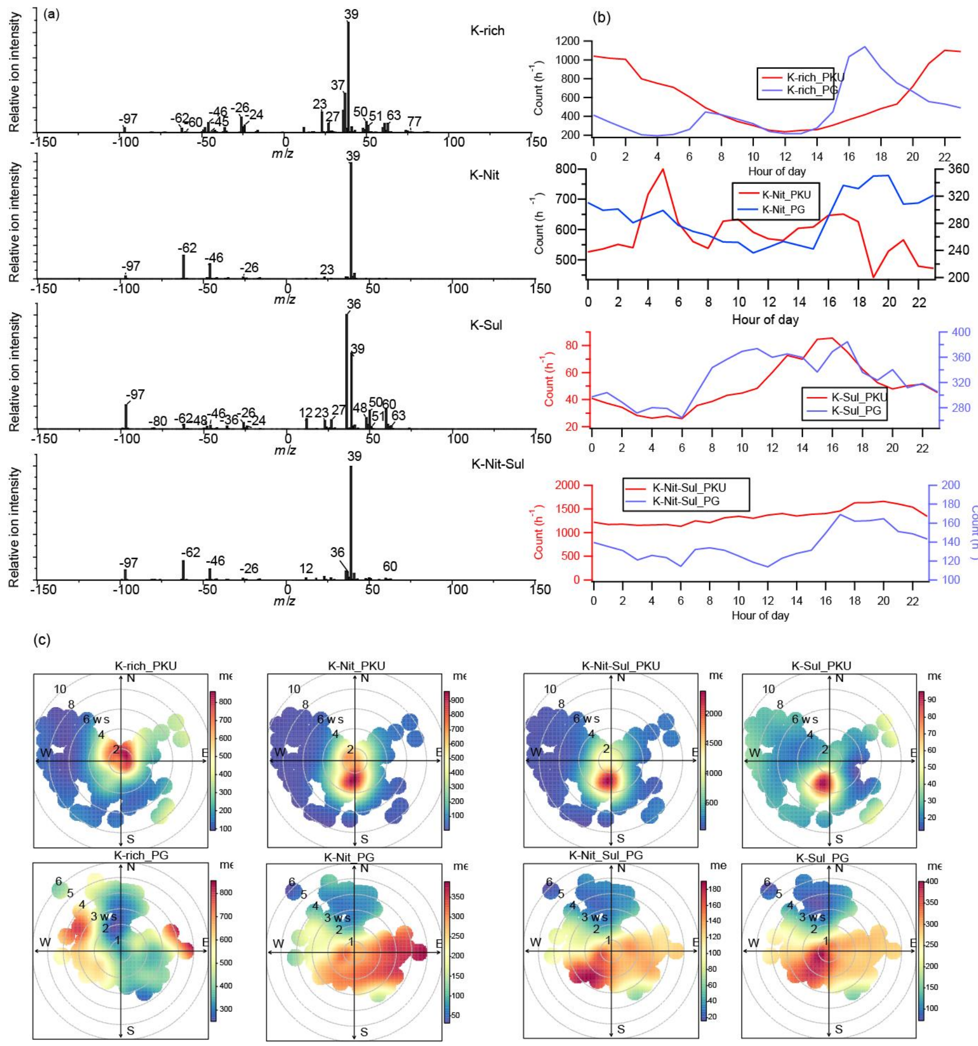

Figure 6. (a): average mass spectra of BB, K-Nit, K-Sul, and K-Nit-Sul observed at both sites; (b): diurnal patterns of the hourly count of K-rich, K-Nit, K-Sul, and K-Nit-Sul at both sites; (c): polar plots of BB, K-Nit, K-Sul, and K-Nit-Sul; the grey circles indicate wind speed (m s^{-1}).

https://doi.org/10.5194/acp-2019-933
Preprint. Discussion started: 9 January 2020

3.2.5 Metal category

Two metal-rich particles types were identified, namely Fe-rich and Ca-rich. Fe-rich contained iron (*m*/*z* 56 and 54), K^+, Na^+, NH_4^+, Cl^- (*m*/*z* -35 and -37), sulfate, and nitrate. Ca-rich was composed of Ca^+ (*m*/*z* 40), CaO (*m*/*z* 56), K^-, Na^+, Cl^-, sulfate, and nitrate. As shown in Figure 6b, Ca-rich_PKU (0.4%) and Ca-rich_PG (0.1%) were likely of regional origin with no distinct diurnal variations. Since SiO_2^- or SiO_3^- (*m*/*z* -60 and -76) were not abundant in the Ca-rich particles, they are not likely to come from dust (Silva et al., 2000). According to its weak peaks during the rush hour at PKU, a possible source of the Ca-rich particles was from road dust re-suspension. Such rush hour peaks were not observed at PG.

Fe-rich_PKU (3.1%) and Fe-rich_PG (1.8%) had similar diurnal profiles that arose in the early morning when heavy-duty vehicles were allowed to enter the 5-ring expressway. The peak occurred earlier at PG (4:00) than (5:00) because these vehicles got close to PG earlier than to PKU. The daytime peak occurred in the afternoon at both PKU and PG when wind speed was high. Therefore, there were also multiple sources for Fe-rich particles, including re-suspended dust particles from traffic and fly ash from the steel industry. In Beijing, daytime Fe-rich particles were reported and assigned to long-range transport and industrial sources from Heibei Province (Figure 7c) (Li et al., 2014). The steel industry moved out of Beijing more than a decade ago (Liu et al., 2016b). Currently, most of these steel industries were located in the Heibei Province.

https://doi.org/10.5194/acp-2019-933
Preprint. Discussion started: 9 January 2020

Atmospheric Chemistry and Physics Discussions
Open Access
EGU

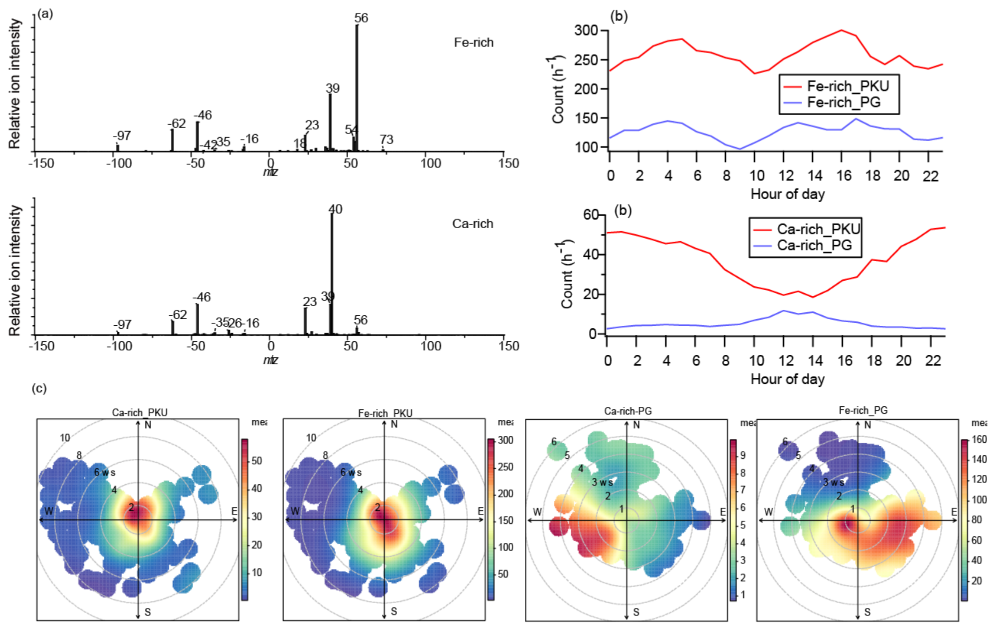

Figure 7. (a): average mass spectra of Fe-rich and Ca-rich observed at both sites; (b): diurnal patterns of the hourly count of Fe-rich and Ca-rich at both sites; (c): polar plots of Fe-rich and Ca-rich; the grey circles indicate wind speed (ms^{-1}).

3.2.6 NaK category

As shown in Figure 8, mass spectra of NaK category contained f Na^+, K^+, C_n^+, C_n^-, nitrate, and PO_3^- (*m/z* -79). The aged NaK particles contained strong signals of nitrate (NaK-Nit), sulfate (NaK-Sul), or both (NaK-Nit-Sul). In general, the NaK category contained stronger signals of Na^+ than the EC and K-rich categories. The NaK category may also come from incomplete solid fuel combustion processes such as coal, peat, or wood (Chen et al., 2017; Healy et al., 2010; Xu et al., 2017). NaK category was more abundant at PKU (9.5%) than PG (5.8%), suggesting a stronger contribution of emission from coal boilers (Xu et al.,

https://doi.org/10.5194/acp-2019-933
Preprint. Discussion started: 9 January 2020

2017; Xu et al., 2018). Additionally, after heating began, the fraction of NaK-Nit_PG and NaK-Sul-Nit_PG increased by 1.2 times (see Part II).

NaK_PKU showed no distinct diurnal variations, suggesting that it was a regional particle type arriving at the PKU site via transport, while NaK_PG showed an apparent diurnal variation consistent with cooking and heating pattern. Polar plots also suggest that they are from the east and the west. NaK-Nit, with a considerable uptake of nitrate, was more abundant at PKU (6.4%) than PG (1.7%). Both NaK-Nit_PKU and NaK-Nit _PG increased in the afternoon when photochemical activities were most active (Figure 8c). Both of them may be from regional transport (Figures 8b and 8c).

NaK-Sul was a minor particle type at both PG and PKU, accounting for 0.2% and 0.4%, respectively. The diurnal profile of NaK-Sul_PG was also following the local cooking and heating pattern, while NaK-Sul_PKU showed a typical transport pattern that became abundant in the afternoon as the southwestern wind speed increased. As a heavily aged particle type, NaK-Nit-Sul was transported to both PKU and PG from the southwest. In short, NaK-related particle types mainly came from the solid fuel burning process, e.g., coal. Due to its different origins, it showed different levels of processing at PKU and PG, respectively.

https://doi.org/10.5194/acp-2019-933
Preprint. Discussion started: 9 January 2020

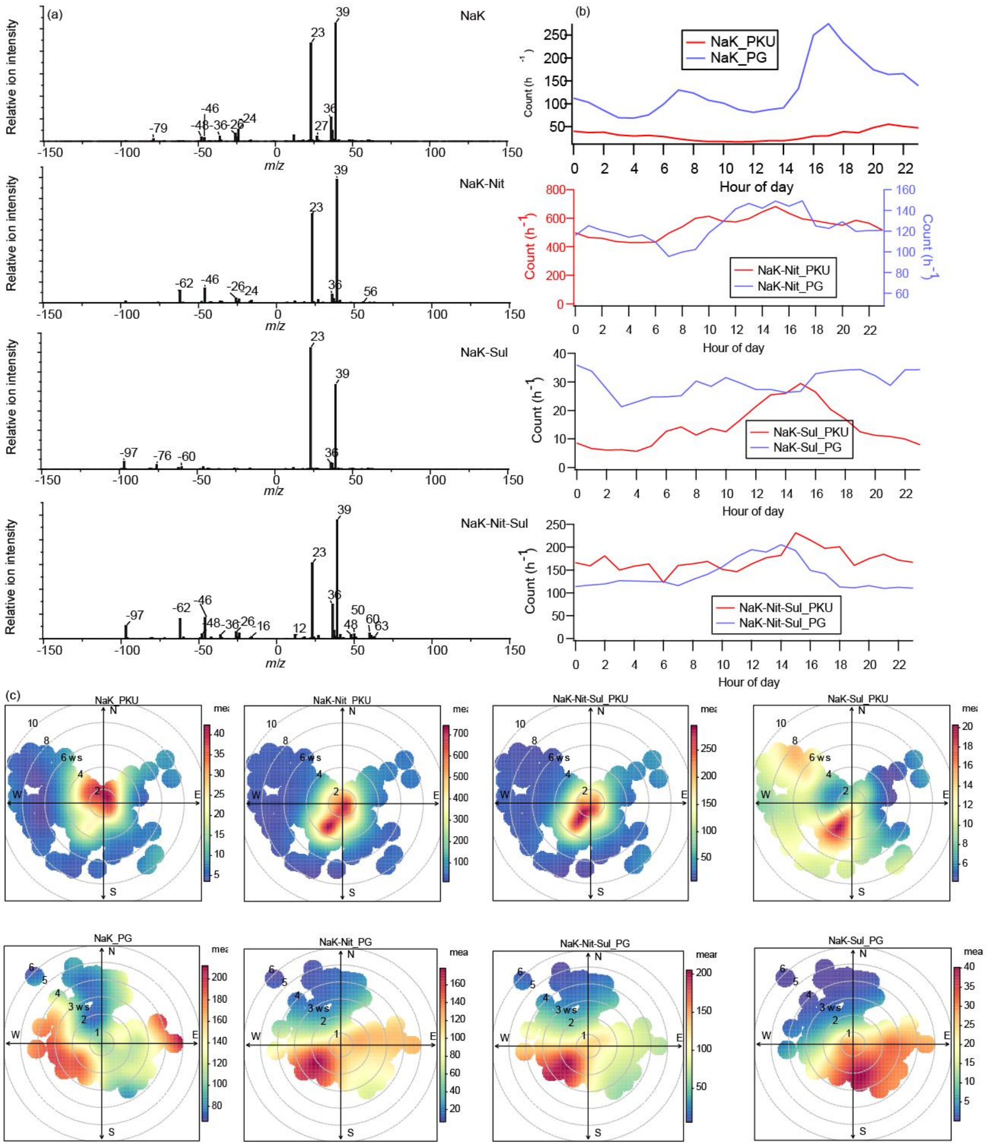

Figure 8. (a): average mass spectra of NaK, NaK-Nit, NaK-Nit-Sul, and NaK-Sul observed at both sites; (b): diurnal patterns of the hourly count of NaK, NaK-Nit, NaK-Nit-Sul, and NaK-Sul at both sites; (c): polar plots of NaK, NaK-Nit, NaK-Nit-Sul, and NaK-Sul; the grey circles indicate wind speed (m s^{-1}).

https://doi.org/10.5194/acp-2019-933
Preprint. Discussion started: 9 January 2020

3.3 Unique Particle types at the PKU site

OC-Nit_PKU (0.9%) and ECOC-Nit_PKU (3.1%) with strong ion intensities of nitrate were observed at the PKU site. OC-Nit_PKU and ECOC-Nit_PKU showed a peak at night than at daytime, similar to the diurnal profiles of OC-Nit-Sul_PKU and ECOC-Nit-Sul_PKU. Such nitrate-rich particle types could have come from the uptake of nitrate in OC and ECOC(Qin et al., 2012; Chen et al., 2016). Polar plots suggest that both types were formed locally when the wind speed was lower than 4 ms^{-1}. The NO_x-rich environment in urban Beijing provides a favorable condition for nitrate formation at night (Wang et al., 2016; Zou et al., 2015; Shi et al., 2019).

A minor amount (0.10%) of amine-containing particles was observed at the PKU site, and trimethylamine ion fragments (*m*/*z* 58 and 59) were influential in the mass spectrum of K-amine-Nit-Sul_PKU (Figure 9a). The diurnal profile of K-amine-Nit-Sul_PKU showed an afternoon peak, indicating a regional source (Figure 9c). K-amine-Nit-Sul_PKU was transported to the site from nearby locations. The amines may come from animal husbandry, BB, traffic, or vegetation (Chen et al., 2019). Amines were ubiquitous in the atmospheric environment, playing essential roles in new particle formation and growth, as well as fog and cloud processing (Ge et al., 2011; Chen et al., 2019).

https://doi.org/10.5194/acp-2019-933
Preprint. Discussion started: 9 January 2020

341 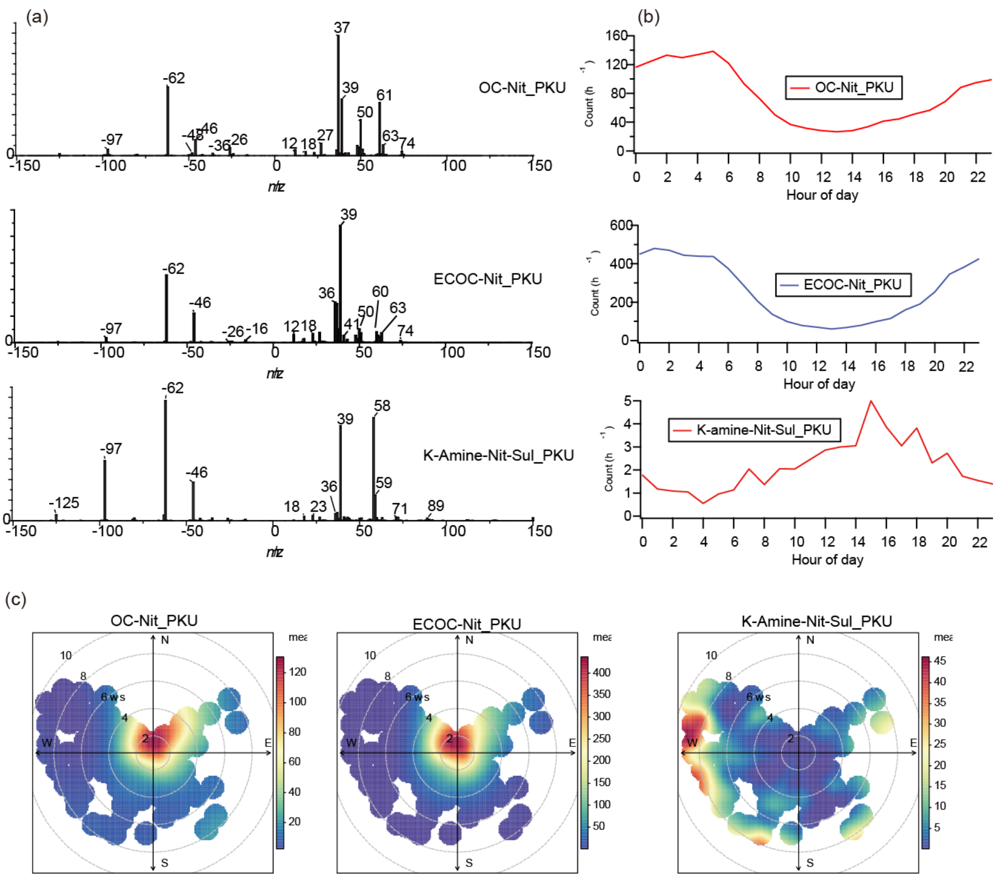

342 Figure 9. (a): average mass spectra of OC-Nit_PKU, ECOC-Nit_PKU, and K-amine-Nit-
343 Sul_PKU observed at the PKU site; (b): diurnal patterns of the hourly count of OC-
344 Nit_PKU, ECOC-Nit_PKU, and K-amine-Nit-Sul_PKU at the PKU site; (c): polar plots of
345 OC-Nit_PKU, ECOC-Nit_PKU, and K-amine-Nit-Sul_PKU, and the grey circles indicate
346 wind speed (m s^{-1}).

347 **3.4 Unique Particle types at the PG site**

348 OC_PG (5.9%) and ECOC_PG (3.3%) were only observed at the rural site PG (Figure 10).
349 The major components of these two types were consistent with the OC and ECOC

categories, respectively, but with limited uptake of sulfate and nitrate, suggesting that they were possibly freshly emitted particles. Their diurnal profiles are consistent with cooking and heating patterns which peaked at 07:00 in the morning and 17:00. Polar plots suggest that OC_PG mainly came from nearby and other remote areas in all directions except the north. ECOC mainly came from the east of the PG site. These results supported the assumption that the two types were mainly from local emission sources.

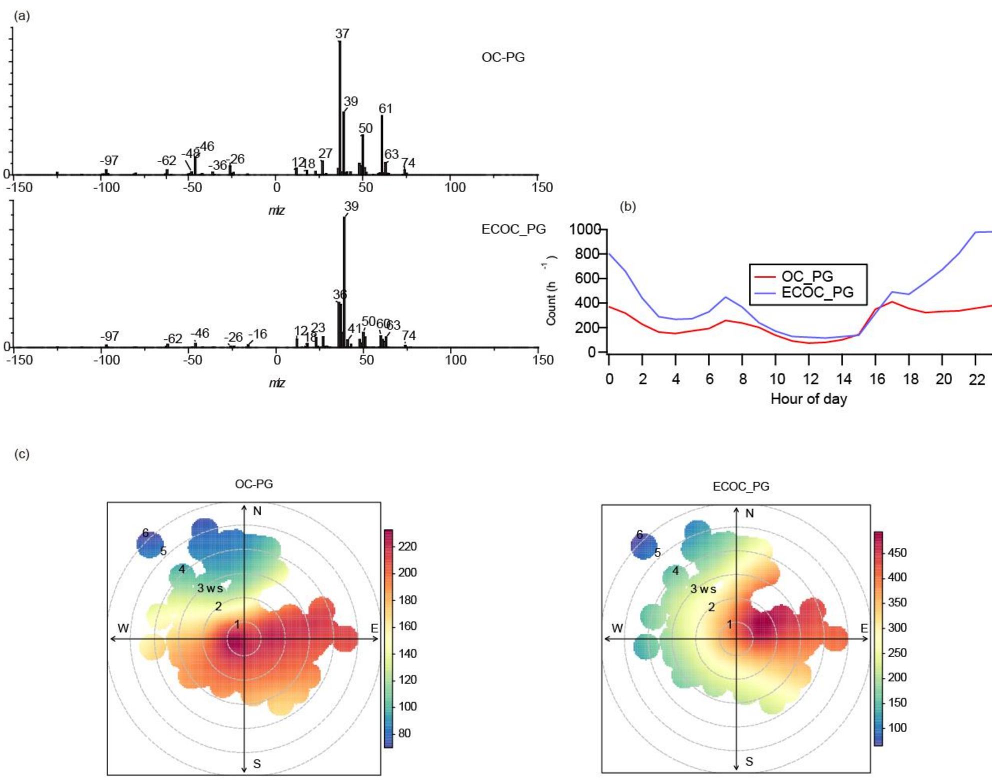

Figure 10. Average mass spectra of (a) ECOC-Nit, (b) ECOC-Nit, and (c) OC-Nit. All these particle types appeared at the PG site.

4. Discussion

Multiple source apportionment models have been used in Beijing to quantify the sources of particles (Sun et al., 2014; Xu et al., 2015; Zhai et al., 2016). Biomass burning, coal combustion, traffic, and dust are the key sources of PM (Sun et al., 2014; Liu et al., 2018; Huang et al., 2014). Multiple studies confirmed that biomass burning is an essential source of PM in urban Beijing (Gao et al., 2014; Huang et al., 2014; Sun et al., 2014; Zheng et al., 2017). In this study, biomass burning, and other solid fuel burning were identified as crucial sources of PM in not only urban but also rural areas of Beijing. We observed that BB-related particles (K-rich category) were more abundant at PG than at PKU. In particular, we found fresh-emitted K-containing particles at the Pinggu site, confirmed the importance of local emissions to PM. Furthermore, K-containing particles in the urban area were more aged, suggested that they are aged and mostly from the surrounding areas. The result is consistent with the results from (Liu et al., 2019) based on a combined receptor and footprint models. Nevertheless, household emissions in the BHT region caused 32% and 15% of primary $PM_{2.5}$ and SO_2. These studies have proved the importance of household emission from BB in the BHT area (Liu et al., 2016a). Especially at the PG site, the ambient PM was mainly controlled by long-range transport and household emissions from cooking and heating.

Due to the nature of SPAMS, the chemical composition of PM cannot be precisely quantified. However, single particle aerosol mass spectrometers have advantages in studying the chemical composition, mixing state, source, and process of particles (Pratt and Prather, 2012). Mass-based technologies can not differentiate the origin of the bulk of nitrate, whether it is transported or formed locally. Indeed, single particle types in urban

https://doi.org/10.5194/acp-2019-933
Preprint. Discussion started: 9 January 2020

Beijing have been reported in previous studies (Li et al., 2014; Liu et al., 2016b), and the major types are consistent with this study. However, in this study, we adopted a cluster strategy considering the relative ion peak area of sulfate and nitrate as indicators of particle processing. Therefore, more detailed could be extracted from both two simultaneous datasets. We confirmed that the source, origination, and processes were different for these particles in the urban and rural areas. For example, the seriously processed particles, such as K-Nit-Sul, OC-Nit-Sul, and NaK-Nit-Sul, acted with no distinct diurnal patterns as background or regional sources. The processed particles, such as OC-Nit, ECOC-Nit, and NaK-Nit, were affected by emissions and secondary formations.

The emission and transport patterns were different in the urban and rural areas, resulting in different characteristics of PM. For example, EC particles were a key component at PKU (18.2% in total), but a minor particle type at PG (5.6%). Meanwhile, in the urban area of Beijing, direct emission of K-rich particles should be small due to strict control measures; thus, the K-Nit-Sul particles are mainly from long-range transport. More interestingly, the sulfate-rich particle types, such as EC-Sul and ECOC-Sul, were commonly accompanied by high wind speed, suggesting the contribution of regional air masses. Sulfate and SO_2 emissions were controlled strictly in Beijing. However, in the nearby Hebei and Shandong province, the emission of SO_2 is still significant (Shi et al. 2019). Transported particles were aged and commonly coated a thick layer of nitrate and sulfate, but the local particles were affected by both emission and the near-surface aging process. For example, at PKU, the primary emission sources were traffic and central heating supply, causing a NO_x-rich region in which freshly-emitted particle types could undergo processing due to the uptake of nitrate (Wang et al., 2016). In the nearby villages of PG, domestic heating and cooking

https://doi.org/10.5194/acp-2019-933
Preprint. Discussion started: 9 January 2020

Atmospheric Chemistry and Physics Discussions

were the major contributors of primary particles when the temperature was low in the morning and afternoon, resulting in the emission of multiple primary particle types such as OC_PG and ECOC_PG. In short, the characteristics of PM in urban and rural areas of Beijing were affected by local emissions and interacted with each other due to regional transport.

Secondary nitrate formation is still a critical issue in Beijing. The daytime arising of nitrate has been reported in studies (Sun et al., 2013), and we also found a similar predominant of nitrogen-containing particles in this study. Recent studies have reported the early morning peaks of nitrate using a soot particle aerosol mass spectrometer (SP-AMS) (Wang et al., 2019), which is consistent with our results. Interestingly, the early morning peak was only observed for several particle types at both sites, including EC-Nit_PKU, K-Nit_PKU, EC-Nit-Sul-PG, and EC-Nit_PG. This result is not surprising because PG is also a NO_2-rich region (Shi et al., 2019). The increasing contribution of nitrate-containing particles suggests the role of night chemistry in nitrate uptake on particles. Wang et al. (2017) revealed the importance of night N_2O_5 chemistry on nocturnal nitrate formation in the urban area of Beijing. The heterogeneous hydrolysis of N_2O_5 was most favorable when NO was at a low level. Moreover, the polar plots suggested a small role of long-range transport to the nitrate in individual particles. The contribution of local traffic was insignificant at the PG site as it was far from highways and major roads, the nighttime formation of nitrate appeared to be important in PG as well.

https://doi.org/10.5194/acp-2019-933
Preprint. Discussion started: 9 January 2020

Atmospheric Chemistry and Physics
Discussions

5. Conclusion

Two SPAMSs were simultaneously deployed at urban and rural sites in Beijing in order to characterize PM during wintertime. The results at both sites indicate that they shared 17 types of common clusters, most of which belonged to particle categories such as EC, OC, ECOC, BB, and NaK. The origins and sources of these particle types at both sampling sites are also comprehensively analyzed. Most of the processed PM, including EC-Nit-Sul_PKU, ECOC-Nit-Sul_PKU, and NaK-Nit-Sul_PKU, were aged locally in a NO_x-rich environment, while EC-Nit-Sul_PG, ECOC-Nit-Sul_PG, NaK-Nit-Sul_PG, and OC-Nit-Sul_PG were regional. Domestic heating in the rural area was found to be an important source of PM, and such heating activities typically caused three diurnal peaks in the early morning, morning, and afternoon (after sunset). Moreover, the early morning peak of nitrate was observed at both sites, suggesting the contribution of the heterogeneous hydrolysis of N_2O_5 in the dark during the winter. The insights gained in this study can provide useful references for understanding the relationship between regional transport and local aging in both urban and rural areas in Beijing. In Part II, we focus on haze events observed at both sites and attempt to determine the effects of heating activities and possible regional transport between PKU and PG.

Data availability. All data described in this study are available upon request from the corresponding authors.

Author contributions. FY, MZ, TZ, QZ, and KH designed the experiments; YC, JC, ZW, MT, CP, and HY carried them out; XYang, XYao, YL, GS, and ZS analyzed the experimental data; YC prepared the manuscript with contributions from all coauthors.

https://doi.org/10.5194/acp-2019-933
Preprint. Discussion started: 9 January 2020

Competing interests. The authors declare that they have no conflict of interest.

Acknowledgments. We are grateful for financial support from the National Natural Science Foundation of China (Grant No. 4170030287 and 81571130100). ZS acknowledges funding from NERC (NE/N007190/1 and NE/R005281/1).

References

Bi, X. H., Zhang, G. H., Li, L., Wang, X. M., Li, M., Sheng, G. Y., Fu, J. M., and Zhou, Z.: Mixing state of biomass burning particles by single particle aerosol mass spectrometer in the urban area of PRD, China, Atmos Environ, 45, 3447-3453, 10.1016/j.atmosenv.2011.03.034, 2011.

Cai, J., Wang, J., Zhang, Y., Tian, H., Zhu, C., Gross, D. S., Hu, M., Hao, J., He, K., and Wang, S.: Source apportionment of Pb-containing particles in Beijing during January 2013, Environ Pollut, 226, 30-40, 2017.

Chen, Y., Cao, J., Huang, R., Yang, F., Wang, Q., and Wang, Y.: Characterization, mixing state, and evolution of urban single particles in Xi'an (China) during wintertime haze days, Sci Total Environ, 573, 937-945, 10.1016/j.scitotenv.2016.08.151, 2016.

Chen, Y., Wenger, J. C., Yang, F., Cao, J., Huang, R., Shi, G., Zhang, S., Tian, M., and Wang, H.: Source characterization of urban particles from meat smoking activities in Chongqing, China using single particle aerosol mass spectrometry, Environ Pollut, 228, 92-101, 10.1016/j.envpol.2017.05.022, 2017.

Chen, Y., Tian, M., Huang, R.-J., Shi, G., Wang, H., Peng, C., Cao, J., Wang, Q., Zhang, S., Guo, D., Zhang, L., and Yang, F.: Characterization of urban amine-containing particles

https://doi.org/10.5194/acp-2019-933
Preprint. Discussion started: 9 January 2020

in southwestern China: seasonal variation, source, and processing, Atmos. Chem. Phys., 19, 3245-3255, 10.5194/acp-19-3245-2019, 2019.

Dall'Osto, M., Beddows, D., McGillicuddy, E. J., Esser-Gietl, J. K., Harrison, R. M., and Wenger, J. C.: On the simultaneous deployment of two single-particle mass spectrometers at an urban background and a roadside site during SAPUSS, Atmos Chem Phys, 16, 9693-9710, 2016.

Dallosto, M., and Harrison, R.: Chemical characterisation of single airborne particles in Athens (Greece) by ATOFMS, Atmos Environ, 40, 7614-7631, 10.1016/j.atmosenv.2006.06.053, 2006.

Day, D. A., Liu, S., Russell, L. M., and Ziemann, P. J.: Organonitrate group concentrations in submicron particles with high nitrate and organic fractions in coastal southern California, Atmos Environ, 44, 1970-1979, 10.1016/j.atmosenv.2010.02.045, 2010.

Du, W., Zhao, J., Wang, Y., Zhang, Y., Wang, Q., Xu, W., Chen, C., Han, T., Zhang, F., Li, Z., Fu, P., Li, J., Wang, Z., and Sun, Y.: Simultaneous measurements of particle number size distributions at ground level and 260 m on a meteorological tower in urban Beijing, China, Atmos Chem Phys, 17, 6797-6811, 10.5194/acp-17-6797-2017, 2017.

Gao, J., Zhang, Y., Zhang, M., Zhang, J., Wang, S., Tao, J., Wang, H., Luo, D., Chai, F., and Ren, C.: Photochemical properties and source of pollutants during continuous pollution episodes in Beijing, October, 2011, Journal of Environmental Sciences, 26, 44-53, 10.1016/S1001-0742(13)60379-4, 2014.

https://doi.org/10.5194/acp-2019-933
Preprint. Discussion started: 9 January 2020

Gard, E., Mayer, J. E., Morrical, B. D., Dienes, T., Fergenson, D. P., and Prather, K. A.: Real-time analysis of individual atmospheric aerosol particles: Design and performance of a portable ATOFMS, Anal Chem, 69, 4083-4091, 1997.

Ge, X., Wexler, A. S., and Clegg, S. L.: Atmospheric amines – Part I. A review, Atmos Environ, 45, 524-546, 10.1016/j.atmosenv.2010.10.012, 2011.

Guo, S., Hu, M., Guo, Q., Zhang, X., Zheng, M., Zheng, J., Chang, C. C., Schauer, J. J., and Zhang, R.: Primary sources and secondary formation of organic aerosols in Beijing, China, Environ Sci Technol, 46, 9846-9853, 10.1021/es2042564, 2012.

Guo, S., Hu, M., Zamora, M. L., Peng, J., Shang, D., Zheng, J., Du, Z., Wu, Z., Shao, M., Zeng, L., Molina, M. J., and Zhang, R.: Elucidating severe urban haze formation in China, Proc Natl Acad Sci U S A, 111, 17373-17378, 10.1073/pnas.1419604111, 2014.

He, K., Yang, F., Ma, Y., Zhang, Q., Yao, X., Chan, C. K., Cadle, S., Chan, T., and Mulawa, P.: The characteristics of PM2.5 in Beijing, China, Atmos Environ, 35, 4959-4970, 10.1016/s1352-2310(01)00301-6, 2001.

Healy, R. M., Hellebust, S., Kourtchev, I., Allanic, A., O'Connor, I. P., Bell, J. M., Healy, D. A., Sodeau, J. R., and Wenger, J. C.: Source apportionment of $PM_{2.5}$ in Cork Harbour, Ireland using a combination of single particle mass spectrometry and quantitative semi-continuous measurements, Atmos Chem Phys, 10, 9593-9613, 10.5194/acp-10-9593-2010, 2010.

Healy, R. M., Sciare, J., Poulain, L., Kamili, K., Merkel, M., Muller, T., Wiedensohler, A., Eckhardt, S., Stohl, A., Sarda-Esteve, R., McGillicuddy, E., O'Connor, I. P., Sodeau, J. R., and Wenger, J. C.: Sources and mixing state of size-resolved elemental carbon particles in

https://doi.org/10.5194/acp-2019-933
Preprint. Discussion started: 9 January 2020

a European megacity: Paris, Atmos Chem Phys, 12, 1681-1700, DOI 10.5194/acp-12-1681-2012, 2012.

Huang, M., Hao, L., Guo, X., Hu, C., Gu, X., Zhao, W., Wang, Z., Fang, L., and Zhang, W.: Characterization of secondary organic aerosol particles using aerosol laser time-of-flight mass spectrometer coupled with FCM clustering algorithm, Atmos Environ, 64, 85-94, 10.1016/j.atmosenv.2012.09.044, 2013.

Huang, R. J., Zhang, Y., Bozzetti, C., Ho, K. F., Cao, J. J., Han, Y., Daellenbach, K. R., Slowik, J. G., Platt, S. M., Canonaco, F., Zotter, P., Wolf, R., Pieber, S. M., Bruns, E. A., Crippa, M., Ciarelli, G., Piazzalunga, A., Schwikowski, M., Abbaszade, G., Schnelle-Kreis, J., Zimmermann, R., An, Z., Szidat, S., Baltensperger, U., El Haddad, I., and Prevot, A. S.: High secondary aerosol contribution to particulate pollution during haze events in China, Nature, 514, 218-222, 10.1038/nature13774, 2014.

Huang, X.-F., He, L.-Y., Hu, M., and Zhang, Y.-H.: Annual variation of particulate organic compounds in PM2.5 in the urban atmosphere of Beijing, Atmos Environ, 40, 2449-2458, 10.1016/j.atmosenv.2005.12.039, 2006.

Huang, X. F., He, L. Y., Hu, M., Canagaratna, M. R., Sun, Y., Zhang, Q., Zhu, T., Xue, L., Zeng, L. W., Liu, X. G., Zhang, Y. H., Jayne, J. T., Ng, N. L., and Worsnop, D. R.: Highly time-resolved chemical characterization of atmospheric submicron particles during 2008 Beijing Olympic Games using an Aerodyne High-Resolution Aerosol Mass Spectrometer, Atmos. Chem. Phys., 10, 8933-8945, 10.5194/acp-10-8933-2010, 2010.

Li, L., Huang, Z., Dong, J., Li, M., Gao, W., Nian, H., Fu, Z., Zhang, G., Bi, X., Cheng, P., and Zhou, Z.: Real time bipolar time-of-flight mass spectrometer for analyzing single aerosol particles, Int J Mass Spectrom, 303, 118-124, 10.1016/j.ijms.2011.01.017, 2011.

Li, L., Li, M., Huang, Z., Gao, W., Nian, H., Fu, Z., Gao, J., Chai, F., and Zhou, Z.: Ambient particle characterization by single particle aerosol mass spectrometry in an urban area of Beijing, Atmos Environ, 94, 323-331, 10.1016/j.atmosenv.2014.03.048, 2014.

Li, P., Yan, R., Yu, S., Wang, S., Liu, W., and Bao, H.: Reinstate regional transport of PM2.5 as a major cause of severe haze in Beijing, Proc Natl Acad Sci U S A, 112, E2739-2740, 10.1073/pnas.1502596112, 2015.

Liu, J., Mauzerall, D. L., Chen, Q., Zhang, Q., Song, Y., Peng, W., Klimont, Z., Qiu, X., Zhang, S., Hu, M., Lin, W., Smith, K. R., and Zhu, T.: Air pollutant emissions from Chinese households: A major and underappreciated ambient pollution source, Proceedings of the National Academy of Sciences, 113, 7756-7761, 10.1073/pnas.1604537113, 2016a.

Liu, L., Wang, Y., Du, S., Zhang, W., Hou, L., Vedal, S., Han, B., Yang, W., Chen, M., and Bai, Z.: Characteristics of atmospheric single particles during haze periods in a typical urban area of Beijing: A case study in October, 2014, J Environ Sci (China), 40, 145-153, 10.1016/j.jes.2015.10.027, 2016b.

Liu, Y., Zheng, M., Yu, M., Cai, X., Du, H., Li, J., Zhou, T., Yan, C., Wang, X., Shi, Z., Harrison, R. M., Zhang, Q., and He, K.: High Time Resolution Source Apportionment of PM_{2.5} in Beijing with Multiple Models, Atmospheric Chemistry and Physics Discussions, 2018, 1-31, 10.5194/acp-2018-1234, 2018.

https://doi.org/10.5194/acp-2019-933
Preprint. Discussion started: 9 January 2020

Liu, Y., Zheng, M., Yu, M., Cai, X., Du, H., Li, J., Zhou, T., Yan, C., Wang, X., Shi, Z., Harrison, R. M., Zhang, Q., and He, K.: High-time-resolution source apportionment of PM_{2.5} in Beijing with multiple models, Atmos Chem Phys, 19, 6595-6609, 10.5194/acp-19-6595-2019, 2019.

Ma, L., Li, M., Huang, Z. X., Li, L., Gao, W., Nian, H. Q., Zou, L. L., Fu, Z., Gao, J., Chai, F. H., and Zhou, Z.: Real time analysis of lead-containing atmospheric particles in Beijing during springtime by single particle aerosol mass spectrometry, Chemosphere, 154, 454-462, 10.1016/j.chemosphere.2016.04.001, 2016.

McGuire, M. L., Jeong, C. H., Slowik, J. G., Chang, R. Y. W., Corbin, J. C., Lu, G., Mihele, C., Rehbein, P. J. G., Sills, D. M. L., Abbatt, J. P. D., Brook, J. R., and Evans, G. J.: Elucidating determinants of aerosol composition through particle-type-based receptor modeling, Atmos Chem Phys, 11, 8133-8155, 10.5194/acp-11-8133-2011, 2011.

Pagels, J., Dutcher, D. D., Stolzenburg, M. R., McMurry, P. H., Gälli, M. E., and Gross, D. S.: Fine-particle emissions from solid biofuel combustion studied with single-particle mass spectrometry: Identification of markers for organics, soot, and ash components, Journal of Geophysical Research: Atmospheres, 118, 859-870, 10.1029/2012jd018389, 2013.

Pratt, K. A., and Prather, K. A.: Mass spectrometry of atmospheric aerosols--recent developments and applications. Part II: On-line mass spectrometry techniques, Mass Spectrom Rev, 31, 17-48, 10.1002/mas.20330, 2012.

Qin, X. Y., Pratt, K. A., Shields, L. G., Toner, S. M., and Prather, K. A.: Seasonal comparisons of single-particle chemical mixing state in Riverside, CA, Atmos Environ, 59, 587-596, 10.1016/j.atmosenv.2012.05.032, 2012.

https://doi.org/10.5194/acp-2019-933
Preprint. Discussion started: 9 January 2020

Atmospheric Chemistry and Physics Discussions

Shi, Z., Vu, T., Kotthaus, S., Harrison, R. M., Grimmond, S., Yue, S., Zhu, T., Lee, J., Han, Y., Demuzere, M., Dunmore, R. E., Ren, L., Liu, D., Wang, Y., Wild, O., Allan, J., Acton, W. J., Barlow, J., Barratt, B., Beddows, D., Bloss, W. J., Calzolai, G., Carruthers, D., Carslaw, D. C., Chan, Q., Chatzidiakou, L., Chen, Y., Crilley, L., Coe, H., Dai, T., Doherty, R., Duan, F., Fu, P., Ge, B., Ge, M., Guan, D., Hamilton, J. F., He, K., Heal, M., Heard, D., Hewitt, C. N., Hollaway, M., Hu, M., Ji, D., Jiang, X., Jones, R., Kalberer, M., Kelly, F. J., Kramer, L., Langford, B., Lin, C., Lewis, A. C., Li, J., Li, W., Liu, H., Liu, J., Loh, M., Lu, K., Lucarelli, F., Mann, G., McFiggans, G., Miller, M. R., Mills, G., Monk, P., Nemitz, E., O'Connor, F., Ouyang, B., Palmer, P. I., Percival, C., Popoola, O., Reeves, C., Rickard, A. R., Shao, L., Shi, G., Spracklen, D., Stevenson, D., Sun, Y., Sun, Z., Tao, S., Tong, S., Wang, Q., Wang, W., Wang, X., Wang, X., Wang, Z., Wei, L., Whalley, L., Wu, X., Wu, Z., Xie, P., Yang, F., Zhang, Q., Zhang, Y., Zhang, Y., and Zheng, M.: Introduction to the special issue "In-depth study of air pollution sources and processes within Beijing and its surrounding region (APHH-Beijing)", Atmos. Chem. Phys., 19, 7519-7546, 10.5194/acp-19-7519-2019, 2019.

Silva, P. J., Liu, D.-Y., Noble, C. A., and Prather, K. A.: Size and Chemical Characterization of Individual Particles Resulting from Biomass Burning of Local Southern California Species, Environ Sci Technol, 33, 3068-3076, 10.1021/es980544p, 1999.

Silva, P. J., Carlin, R. A., and Prather, K. A.: Single particle analysis of suspended soil dust from Southern California, Atmos Environ, 34, 1811-1820, 10.1016/S1352-2310(99)00338-6, 2000.

https://doi.org/10.5194/acp-2019-933
Preprint. Discussion started: 9 January 2020

Sodeman, D. A., Toner, S. M., and Prather, K. A.: Determination of single particle mass spectral signatures from light-duty vehicle emissions, Environ Sci Technol, 39, 4569-4580, 10.1021/es0489947, 2005.

Sullivan, R. C., Guazzotti, S. a., Sodeman, D. a., Tang, Y., Carmichael, G. R., and Prather, K. a.: Mineral dust is a sink for chlorine in the marine boundary layer, Atmos Environ, 41, 7166-7179, 10.1016/j.atmosenv.2007.05.047, 2007.

Sun, Y., Jiang, Q., Wang, Z., Fu, P., Li, J., Yang, T., and Yin, Y.: Investigation of the sources and evolution processes of severe haze pollution in Beijing in January 2013, J Geophys Res, 119, 4380-4398, 2014.

Sun, Y. L., Wang, Z. F., Fu, P. Q., Yang, T., Jiang, Q., Dong, H. B., Li, J., Jia, J. J., Eskes, H. J., Boersma, K. F., Hussein, T., Puustinen, A., Aalto, P. P., Mäkelä, J. M., Hämeri, K., and Kulmala, M.: Aerosol composition, sources and processes during wintertime in Beijing, China, Atmos. Chem. Phys. Discuss., 13, 4577-4592, 10.5194/acp-13-4577-2013, 2013.

Tao, S., Wang, X., Chen, H., Yang, X., Li, M., Li, L., and Zhou, Z.: Single particle analysis of ambient aerosols in Shanghai during the World Exposition, 2010: two case studies, Front Environ Sci En, 5, 391-401, 10.1007/s11783-011-0355-x, 2011.

Toner, S. M., Sodeman, D. a., and Prather, K. a.: Single particle characterization of ultrafine and accumulation mode particles from heavy duty diesel vehicles using aerosol time-of-flight mass spectrometry, Environ Sci Technol, 40, 3912-3921, 2006.

Toner, S. M., Shields, L. G., Sodeman, D. A., and Prather, K. A.: Using mass spectral source signatures to apportion exhaust particles from gasoline and diesel powered vehicles

https://doi.org/10.5194/acp-2019-933
Preprint. Discussion started: 9 January 2020

Atmospheric Chemistry and Physics Discussions
Open Access

in a freeway study using UF-ATOFMS, Atmos Environ, 42, 568-581, 10.1016/j.atmosenv.2007.08.005, 2008.

Wang, G., Zhang, R., Gomez, M. E., Yang, L., Levy Zamora, M., Hu, M., Lin, Y., Peng, J., Guo, S., Meng, J., Li, J., Cheng, C., Hu, T., Ren, Y., Wang, Y., Gao, J., Cao, J., An, Z., Zhou, W., Li, G., Wang, J., Tian, P., Marrero-Ortiz, W., Secrest, J., Du, Z., Zheng, J., Shang, D., Zeng, L., Shao, M., Wang, W., Huang, Y., Wang, Y., Zhu, Y., Li, Y., Hu, J., Pan, B., Cai, L., Cheng, Y., Ji, Y., Zhang, F., Rosenfeld, D., Liss, P. S., Duce, R. A., Kolb, C. E., and Molina, M. J.: Persistent sulfate formation from London Fog to Chinese haze, Proc Natl Acad Sci U S A, 113, 13630-13635, 10.1073/pnas.1616540113, 2016.

Wang, H., Zhu, B., Zhang, Z., An, J., and Shen, L.: Mixing state of individual carbonaceous particles during a severe haze episode in January 2013, Nanjing, China, Particuology, 20, 16-23, 10.1016/j.partic.2014.06.013, 2015.

Wang, H., Lu, K., Chen, X., Zhu, Q., Chen, Q., Guo, S., Jiang, M., Li, X., Shang, D., Tan, Z., Wu, Y., Wu, Z., Zou, Q., Zheng, Y., Zeng, L., Zhu, T., Hu, M., and Zhang, Y.: High N2O5 Concentrations Observed in Urban Beijing: Implications of a Large Nitrate Formation Pathway, Environ Sci Tech Let, 4, 416-420, 10.1021/acs.estlett.7b00341, 2017.

Wang, H., Lu, K., Chen, X., Zhu, Q., Wu, Z., Wu, Y., and Sun, K.: Fast particulate nitrate formation via N₂O₅ uptake aloft in winter in Beijing, Atmos Chem Phys, 18, 10483-10495, 10.5194/acp-18-10483-2018, 2018.

Wang, J., Liu, D., Ge, X., Wu, Y., Shen, F., Chen, M., Zhao, J., Xie, C., Wang, Q., Xu, W., Zhang, J., Hu, J., Allan, J., Joshi, R., Fu, P., Coe, H., and Sun, Y.: Characterization of black carbon-containing fine particles in Beijing during wintertime, Atmos. Chem. Phys., 19, 447-458, 10.5194/acp-19-447-2019, 2019.

Xu, J., Li, M., Shi, G., Wang, H., Ma, X., Wu, J., Shi, X., and Feng, Y.: Mass spectra features of biomass burning boiler and coal burning boiler emitted particles by single particle aerosol mass spectrometer, Sci Total Environ, 598, 341-352, https://doi.org/10.1016/j.scitotenv.2017.04.132, 2017.

Xu, J., Wang, H., Li, X., Li, Y., Wen, J., Zhang, J., Shi, X., Li, M., Wang, W., Shi, G., and Feng, Y.: Refined source apportionment of coal combustion sources by using single particle mass spectrometry, Sci Total Environ, 627, 633-646, 10.1016/j.scitotenv.2018.01.269, 2018.

Xu, W. Q., Sun, Y. L., Chen, C., Du, W., Han, T. T., Wang, Q. Q., Fu, P. Q., Wang, Z. F., Zhao, X. J., Zhou, L. B., Ji, D. S., Wang, P. C., and Worsnop, D. R.: Aerosol composition, oxidation properties, and sources in Beijing: results from the 2014 Asia-Pacific Economic Cooperation summit study, Atmos. Chem. Phys., 15, 13681-13698, 10.5194/acp-15-13681-2015, 2015.

Zhai, J. H., Wang, X. N., Li, J. Y., Xu, T. T., Chen, H., Yang, X., and Chen, J. M.: Thermal desorption single particle mass spectrometry of ambient aerosol in Shanghai, Atmos Environ, 123, 407-414, 10.1016/j.atmosenv.2015.09.001, 2015.

Zhai, S., An, X., Zhao, T., Sun, Z., Hou, Q., and Wang, C.: Detecting critical PM_{2.5} emission sources and their contributions to a heavy haze episode in Beijing, China by using an adjoint model, Atmospheric Chemistry and Physics Discussions, 2016, 1-20, 10.5194/acp-2016-911, 2016.

https://doi.org/10.5194/acp-2019-933
Preprint. Discussion started: 9 January 2020

Atmospheric Chemistry and Physics Discussions
Open Access
EGU

Zheng, M., Yan, C. Q., Wang, S. X., He, K. B., and Zhang, Y. H.: Understanding PM2.5 sources in China: challenges and perspectives, Natl Sci Rev, 4, 801-803, 10.1093/nsr/nwx129, 2017.

Zou, Y., Deng, X. J., Zhu, D., Gong, D. C., Wang, H., Li, F., Tan, H. B., Deng, T., Mai, B. R., Liu, X. T., and Wang, B. G.: Characteristics of 1 year of observational data of VOCs, NO_{<i>x</i>} and O₃ at a suburban site in Guangzhou, China, Atmos Chem Phys, 15, 6625-6636, 10.5194/acp-15-6625-2015, 2015.